
Biodistribution and Dosimetry of Pretargeted Monoclonal Antibody 2D12.5 and Y-Janus-DOTA in BALB/c Mice with KHJJ Mouse Adenocarcinoma

Stephen P. Lubic, David A. Goodwin, Claude F. Meares, Chung Song, Maureen Osen, and Marguerite Hays

Department of Nuclear Medicine, Veterans Affairs Palo Alto Health Care System, Palo Alto; Department of Radiology, Stanford University, Stanford; and Department of Chemistry, University of California at Davis, Davis, California

Biodistribution and dosimetry of ^{88}Y (and equimolar ^{90}Y) Janus-dodecanetetraacetic acid (DOTA) were performed using a three-step pretargeting protocol in BALB/c mice bearing mouse mammary adenocarcinoma (KHJJ) implants. Pretargeting was performed with mouse monoclonal antibody (mAb) 2D12.5 specific for yttrium-DOTA, and the chase was Y-DOTA-human transferrin conjugate. In this article, we report extensive organ dosimetry and the theoretic limits of the radionuclide physical half-life (T_p) for pretargeting. **Methods:** Organ biodistribution data were obtained from bioassays on tissue taken from tumor mice killed at 3, 24, 48, 72, 96, and 120 h after intravenous injection of ^{88}Y -Janus-DOTA. Uptake and retention of ^{88}Y as a function of time were described by nonlinear least squares fits of the tissue data to multiexponential functions. Radiation dose estimates for equivalent molar amounts of ^{90}Y were subsequently derived from these time-integrated functions. **Results:** The results were as follows: rapid blood clearance of ^{88}Y -Janus-DOTA; rapid uptake and slow clearance of ^{88}Y -Janus-DOTA from the tumor over 5 d; rapid clearance from all organs and body; largest radiation absorbed dose (AD) per injected dose of 63.52 (cGy/MBq) to tumor; high therapeutic ratios (AD tumor/AD tissue), particularly for blood and bone; and optimal radionuclide T_p range from 30 min to 10 d. **Conclusion:** Although the absolute concentration of ^{90}Y in the tumor is less using the hapten system than is achieved generally with the chelated radionuclide covalently attached to the mAb, the achievable tumor uptake of radioactivity, coupled with low radioactivity in bone, blood, and other organs, suggests that a three-step pretargeting protocol has considerable promise as a method for ^{90}Y radioimmunotherapy.

Key Words: radioimmunoimaging; radioimmunotherapy; ^{90}Y ; ^{111}In pretargeting; biodistribution; dosimetry; therapeutic ratio

J Nucl Med 2001; 42:670–678

Antibodies have been labeled with radioisotopes and used in both the localization and therapy of cancer (1–6). The development of monoclonal antibodies (mAbs) with high specificity for tumor marker antigens has made this approach very attractive, because of the possibility of delivering radionuclides to a target tumor in vivo with great selectivity (1,7).

Human imaging studies have shown that although maximum human tumor concentrations of radiolabeled mAb are achieved in 1 d, the slow pharmacokinetics requires several days for the background to fall sufficiently for sensitive radioimmunoscintigraphy of tumors (8). Waiting for the optimum imaging time is a strategy made possible using larger amounts of longer half-life diagnostic radionuclides, such as ^{111}In (9). With therapeutic radionuclides, however, this long biologic half-life imposes a high radiation burden on sensitive normal tissues, especially bone marrow and gut, from the large amount of retained radioactivity (10,11).

Among the metallic radionuclides for radioimmunotherapy, ^{90}Y is especially attractive because of its availability, pure high-energy β -emission, and high dose yield per picomole (12). However, ^{90}Y -mAb conjugated with conventional bifunctional chelators, such as the cyclic dianhydride of diethylenetriaminepentaacetic acid (DTPA), produces bone marrow toxicity in mice before curative therapeutic levels in the tumor are reached (13).

Moi et al. (14) and Renn and Meares (15) developed a macrocyclic bifunctional chelating agent, 2-(*p*-nitrobenzyl)-1,4,7,10-tetraazacyclododecane-*N,N',N'',N'''*-tetraacetic acid (DOTA), that holds yttrium with extraordinary stability under physiologic conditions in human serum (16). Stable chelation of ^{90}Y by Janus-DOTA leads to a reduction of free ^{90}Y that potentially could accumulate in bone (17).

Use of a three-step pretargeting technique developed originally for immunoscintigraphy (18) provides a way to get highly selective tumor uptake of ^{90}Y -DOTA with simultaneous minimization of nontarget tissue background (17).

Received May 26, 2000; revision accepted Dec. 11, 2000.
For correspondence or reprints contact: Stephen P. Lubic, PhD, 1316 Alderbrook Lane, San Jose, CA 95129.

Briefly, the antibody and radiolabel are administered separately. The first or pretargeting step consists of administration of mAb to BALB/c mice with KHJJ mouse tumors. Sufficient time (20 h) is allowed for the tumor to equilibrate with blood mAb. At equilibrium, the tumor has as high an mAb concentration as possible. The next step or chase step is the intravenous injection of a large-molecular-weight polyvalent hapten. This procedure leads to the rapid clearance from blood of excess circulating nonradioactive antibody (19). Finally, 1 h after administration of the chase, the radiolabeled hapten–chelate conjugate is given, and mouse organ and tumor assay or whole-body imaging is performed at various times after the addition of the radiolabel (20). Recognizing these principles, Axworthy et al. (21) used the avidin/biotin system to cure human carcinoma xenografts in mice by a single dose of pretargeted ^{90}Y with negligible toxicity.

Substituting the γ -emitting radionuclides ^{88}Y and ^{111}In as tracers for ^{90}Y -Janus-DOTA, we extend our previous analysis (17) to early blood radioactivity levels and a more complete description of the biodistribution and dosimetry of ^{90}Y to tumor, blood, heart, lung, liver, spleen, kidneys, muscle, bone, skin, and gut. ^{88}Y has a physical half-life (T_p) of 106.64 d and decays through both electron capture and positron emission. This decay produces both x-ray and γ -ray emissions, making it suitable for accurate organ assay in a scintillation well counter.

MATERIALS AND METHODS

Organ biodistribution data were obtained from bioassays performed on tissue taken from tumor mice killed at 3, 24, 48, 72, 96, and 120 h after ^{88}Y -Janus-DOTA injection. Uptake and retention of ^{88}Y as a function of time were described by nonlinear least squares fits of the tissue data to multiexponential functions. Radiation dose estimates for equivalent molar amounts of ^{90}Y were derived subsequently from area-under-the-curve (AUC) estimations calculated from these integrated functions (17).

Mouse Tumor Model and Pretargeting Protocol

The KHJJ mouse breast adenocarcinoma was used in these experiments (22). Unlike the more commonly used nude mouse–human tumor system, this model is analogous to tumor imaging in an immunologically competent patient using human mAb. BALB/c mice were used 2 wk after trocar implantation in the flank, at which time the tumors were approximately 0.7 cm in diameter and weighed 558 ± 220 mg (mean \pm SD; $n = 18$).

Pretargeting used three steps. First, 50–100 μg (0.33–0.67 nmol) 2D12.5 were given intravenously to BALB/c mice bearing KHJJ mouse tumors. Enough time (20 h) was allowed for the mAb to leak through the abnormally permeable tumor neovasculature and to equilibrate with the blood mAb to give the maximum tumor concentration. At this time, a multivalent Y-DOTA conjugate of human transferrin (35.4 μg HTr-2IT-BAD-Y, 0.442 nmol HTr, 3.09 nmol BAD-Y: 6/1 hapten/protein) was given intravenously to clear the blood quickly of the excess circulating nonradioactive antibody. One hour after the chase (21 h after mAb), the ^{88}Y -labeled hapten–chelate was given intravenously (33.3 kBq ^{88}Y , 0.744 pmol Y, 0.484 nmol Janus-DOTA).

The equilibrium association constant (K_a), measured by equilibrium dialysis, for the affinity of 2D12.5 and ^{88}Y -DOTA is approximately 10^8 (17). A previous study in this laboratory (17) with ^{111}In , ^{88}Y , ^{67}Ga , and mono- and divalent haptens using the same pretargeting mAb protocol suggested passive tumor uptake of the antibody through leaky capillaries with no organ uptake, because of the presence of cross-reacting antigen elsewhere in the tissues.

Organ Biodistribution

The tumor mice ($n = 3$ per group) were killed 3, 24, 48, 72, 96, and 120 h after ^{88}Y -Janus-DOTA injection. The percentage injected dose per gram (%ID/g) of decay-corrected ^{88}Y -labeled hapten was determined in blood, heart, lungs, liver, spleen, kidneys, tumor, muscle, bone and marrow (femur), skin, and gut. To obtain a better estimation of the early blood clearance of the metal–hapten chelate, a second experiment was performed as described previously, substituting ^{111}In -Janus-DOTA for ^{88}Y -Janus-DOTA and sampling at 0.08, 0.17, 0.25, 0.5, 1.0, 1.5, 2.0, and 2.5 h after injection.

Data Analysis

Uptake and retention of the ^{88}Y - or ^{111}In -Janus-DOTA as a function of time were described by iterative nonlinear least squares fits of the %ID/g tumor and organ data to multiexponential functions using SAAM II (SAAM Institute, Inc., Seattle, WA), which is a simulation, analysis, and modeling software package.

If $f_j(t)$ is defined as the %ID/g of metal–chelate as a function of time, then:

$$f_j(t) = \sum A_j \exp(-\lambda_j t), \quad \text{Eq. 1}$$

where A_j (%ID/g) and λ_j (biologic uptake or decay rate, time^{-1}) are the fitted parameters.

Absorbed Dose Estimates

Radiation absorbed dose (AD) estimates for equivalent molar amounts of ^{90}Y were derived subsequently from AUC estimates. These were derived from the fitted exponential functions describing the biodistribution of the injected ^{88}Y activity and the ^{90}Y physical decay constant. If $f_h(t)$ is defined as ^{90}Y MBq/kg as a function of time, then:

$$f_h(t) = c_1 f_j(t) \exp(-\lambda_p t), \quad \text{Eq. 2}$$

where c_1 is a constant for the conversion of %ID/g to ^{90}Y MBq/kg and λ_p is the ^{90}Y physical decay constant (time^{-1}). Substituting $\sum A_j \exp(-\lambda_j t)$ for $f_j(t)$ gives:

$$f_h(t) = c_1 \sum A_j \exp(-\lambda_j t) \exp(-\lambda_p t) \quad \text{Eq. 3}$$

and

$$f_h(t) = c_1 \sum A_j \exp[-(\lambda_j + \lambda_p)t]. \quad \text{Eq. 4}$$

If the AUC from time zero to infinity is defined as the integral from zero to infinity, then:

$$\text{AUC}_{0 \rightarrow \infty} = \int_0^{\infty} f_h(t) dt, \quad \text{Eq. 5}$$

or

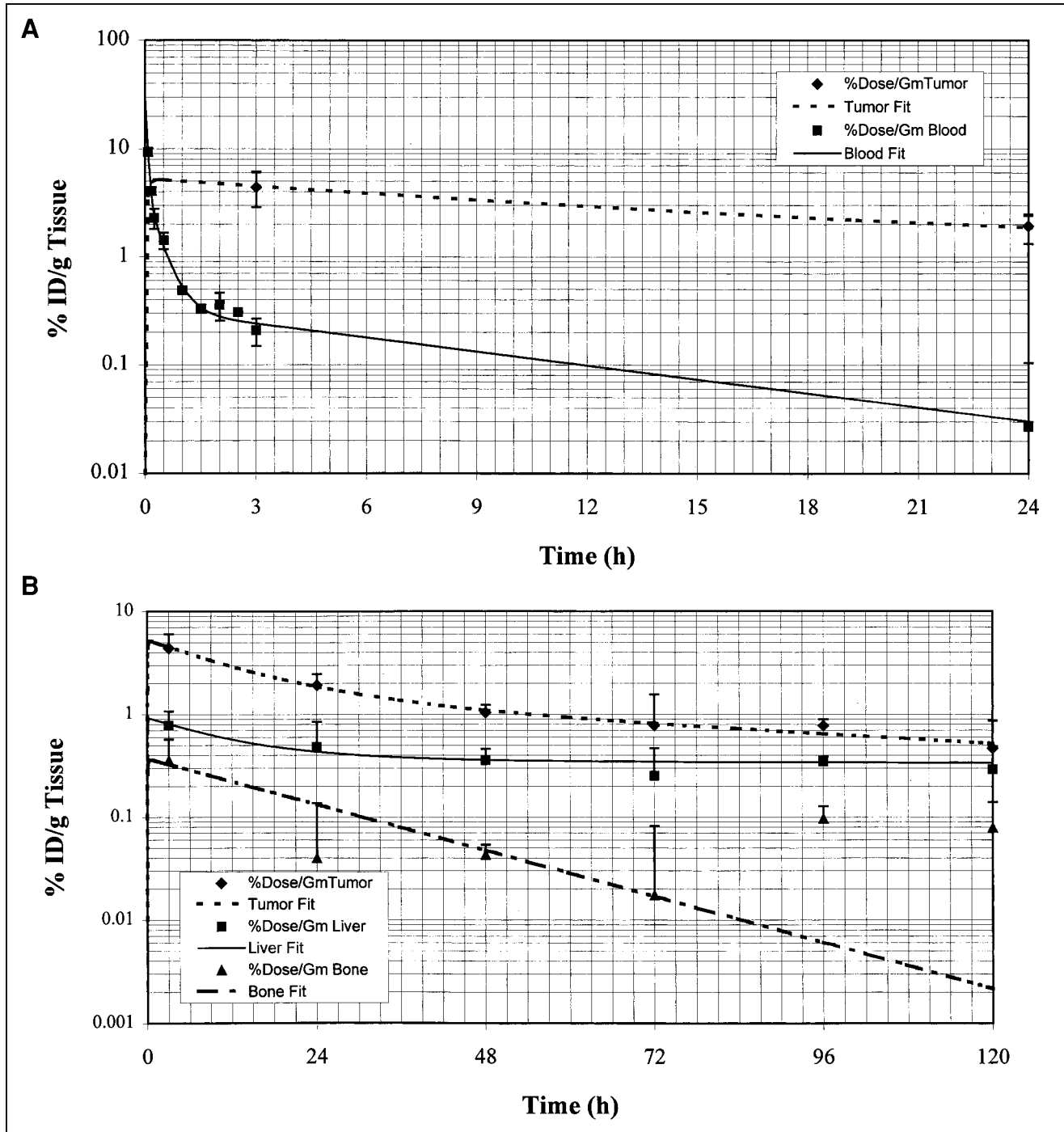


FIGURE 1. (A) Semilog plots of blood (■) clearance of both ^{111}In - (0.08–2.5 h) and ^{88}Y -Janus-DOTA, and tumor (◆) uptake and clearance of ^{88}Y -Janus-DOTA. Note predicted rapid uptake into tumor as blood levels decline rapidly as metal-Janus-DOTA is quickly distributed into interstitial volume. (B) Semilog plots of %ID/g for tumor (◆), liver (■), and bone (▲) predicted uptake and clearance of ^{88}Y -Janus-DOTA. Note much higher initial accumulation in tumor compared with bone and liver.

$$\text{AUC}_{0 \rightarrow \infty} = c_1 \int_0^{\infty} \sum A_j \exp[-(\lambda_j + \lambda_p)t] dt, \quad \text{Eq. 6}$$

Finally, if AD is defined as the product of the AUC from zero to infinity and the energy constant, then:

$$\text{AD} = \text{AUC}_{0 \rightarrow \infty} \times \Delta, \quad \text{Eq. 8}$$

which, when integrated, becomes:

$$\text{AUC}_{0 \rightarrow \infty} = c_1 \sum A_j / (\lambda_j + \lambda_p). \quad \text{Eq. 7}$$

where Δ is the ^{90}Y energy constant (1.49×10^{-5} cGy \times kg/MBq \times s). Then:

TABLE 1
Tumor and Organ 5-Day Biodistribution Data for ⁸⁸Y-Janus-DOTA

Tissue	3 h		24 h		48 h		72 h		96 h		120 h	
	%ID/g	SD										
Blood	0.21	0.06	0.03	0.02	0.05	0.07	0.13	0.23	0.00	0.00	0.00	0.01
Bone	0.35	0.22	0.04	0.10	0.04	0.01	0.02	0.06	0.10	0.03	0.08	0.06
Gut	1.97	1.80	0.36	0.22	0.28	0.03	0.22	0.18	0.46	0.10	0.20	0.30
Heart	0.70	0.38	0.32	0.21	0.25	0.10	0.32	0.32	0.20	0.04	0.21	0.12
Kidneys	1.36	0.27	0.68	0.01	0.67	0.22	0.27	0.23	0.30	0.06	0.25	0.20
Liver	0.78	0.29	0.48	0.36	0.36	0.10	0.25	0.22	0.35	0.04	0.29	0.20
Lung	0.82	0.15	0.43	0.36	0.21	0.09	0.17	0.14	0.11	0.01	0.12	0.10
Muscle	0.56	0.31	0.25	0.08	0.07	0.06	0.06	0.08	0.06	0.03	0.07	0.07
Skin	0.20	0.06	0.12	0.19	0.06	0.06	0.02	0.05	0.04	0.01	0.04	0.02
Spleen	0.23	0.08	0.15	0.10	0.12	0.01	0.10	0.09	0.16	0.05	0.13	0.11
Tumor	4.44	1.63	1.93	0.54	1.04	0.20	0.78	0.77	0.78	0.11	0.47	0.40

Values are mean ± SD for three mice.

$$AD = c_1 \left[\sum A_j / (\lambda_j + \lambda) \right] \times \Delta. \quad \text{Eq. 9}$$

These calculations do not consider the reduction of the dose caused by the escape of energy from the small mouse organs or the effect of such escaped energy on the other organs. Because we are dealing primarily with pure β-emitters, this situation will have little implication for human dosimetry in treatment situations.

Statistics

The AD estimates for the tumor and organs were compared by ANOVA and the Dunnett multiple comparison test, which compared the AD of the tumor to the AD of blood and other tissue (23). In all cases, $P < 0.01$ was considered statistically significant.

RESULTS

Figure 1A is a plot of the %ID/g blood versus time after intravenous injection of ¹¹¹In- and ⁸⁸Y-Janus-DOTA 1 h after injection of the polyvalent hapten–protein conjugate. The data from 0 to 2.5 h are from ¹¹¹In-Janus-DOTA, and

those from 3 to 24 h are from ⁸⁸Y-Janus-DOTA. The data were fitted to the following triexponential function:

$$f_{\%ID/g \text{ blood}}(t) = A_1 \exp(-\lambda_1 t) + A_2 \exp(-\lambda_2 t) + A_3 \exp(-\lambda_3 t), \quad \text{Eq. 10}$$

where A_j (%ID/g) and λ_j (h^{-1}) were the fitted parameters.

The initial blood concentration, C_0 , was 30.06 ± 17.95 %ID/g (mean ± SD), and the estimated volume of distribution (V_D) was 3.3 mL. Both ¹¹¹In- and ⁸⁸Y-Janus-DOTA were cleared rapidly from the blood; only about 0.2 %ID/g remained at 3 h, and <0.03 %ID/g remained at 24 h (Table 1; Fig. 1A).

The uptake and clearance of ⁸⁸Y-Janus-DOTA from the tumor and organs over 5 d is shown in Figure 1B. The tumor data were fitted to the following triexponential function:

$$f_{\%ID/g \text{ tumor}}(t) = A_1 \exp(-\lambda_1 t) + A_2 \exp(-\lambda_2 t) + A_3 \exp(-\lambda_3 t), \quad \text{Eq. 11}$$

where $A_3 = -(A_1 + A_2)$ such that $\sum A_j = 0$ at $t = 0$, and the initial estimate for λ_3 (uptake phase) was obtained from the λ_1 (distribution phase) of the %ID/g blood versus time curve.

Clearance of the metal-DOTA from the tumor was slow compared with the rapid blood clearance. The metal-chelate was bound to the pretargeted antibody in the tumor with 4.44 and 1.93 %ID/g at 3 and 24 h, respectively. This result gave tumor-to-blood ratios of approximately 20:1 and 60:1 at 3 and 24 h, respectively.

The biodistribution data for the remaining organs were fitted to multiexponential equations as above. Figure 1B shows the %ID/g ⁸⁸Y-Janus-DOTA versus time for tumor, liver, and bone. Values of the %ID/g ⁸⁸Y-Janus-DOTA at 3, 24, 48, 72, 96, and 120 h for the tumor and organs are listed in Table 1.

Table 2 summarizes the tumor and organ time-integrated

TABLE 2
Tumor and Organ Time-Integrated Activity and Absorbed Dose for ⁹⁰Y-Janus-DOTA

Tissue	Time-integrated activity (MBq × s/kg)		Absorbed dose (cGy)	
	AUC × 10 ⁻⁵	SD	AD	SD
Blood	2.78	0.56	4.15	0.83
Bone	3.34	0.91	4.99	1.35
Gut	18.79	2.89	28.08	4.32
Heart	12.51	0.97	18.69	1.45
Kidneys	21.70	1.15	32.42	1.71
Liver	18.35	1.35	27.42	2.01
Lung	11.93	0.43	17.83	0.64
Muscle	6.54	0.43	9.77	0.64
Skin	2.56	1.49	3.82	2.22
Spleen	5.75	0.49	8.60	0.74
Tumor	58.83	1.59	87.90	2.37

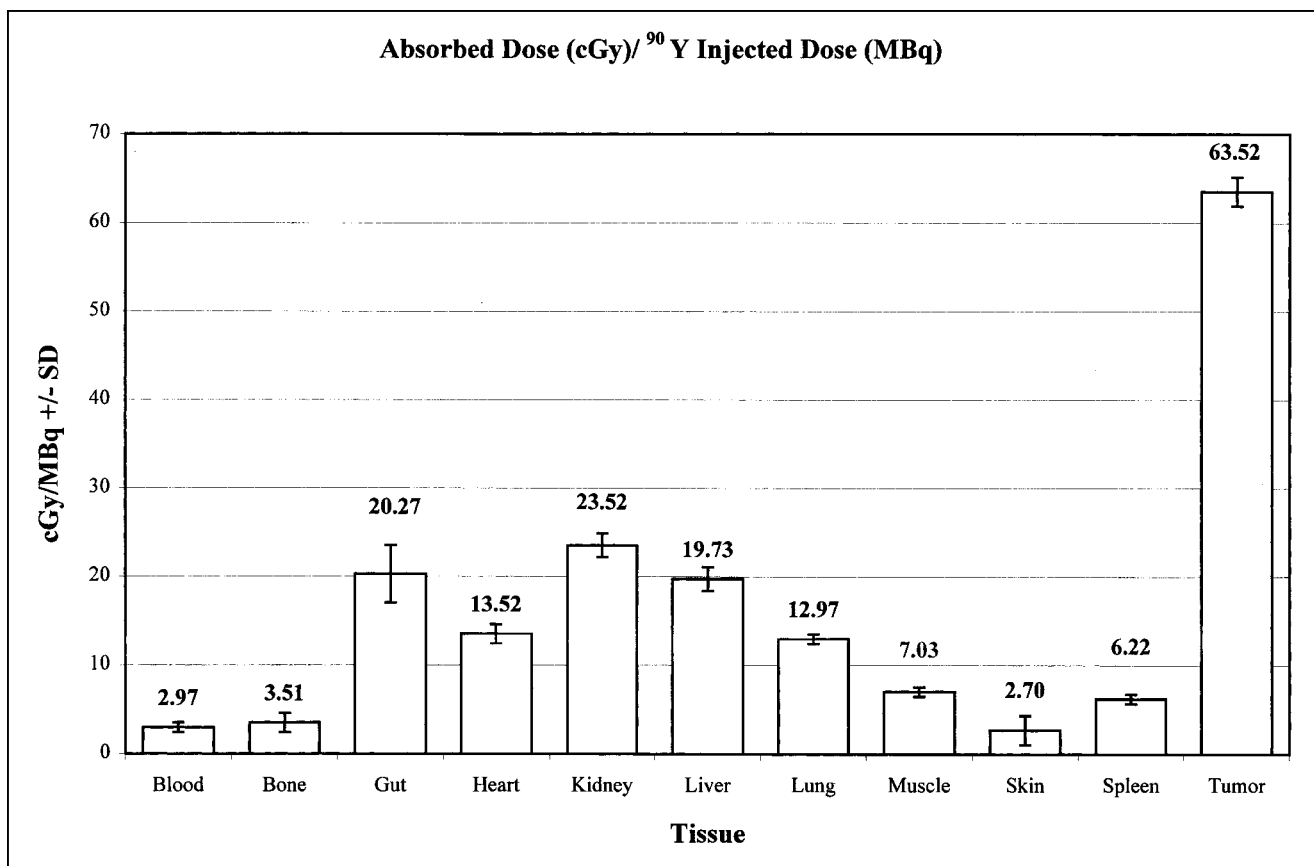


FIGURE 2. Summary of AD (cGy)/injected dose (MBq) ^{90}Y for tumor and organs. The tumor had largest AD compared with all other tissue ($P < 0.01$, ANOVA, Dunnett).

radioactivity (^{90}Y MBq \times s/kg) and AD (cGy) for ^{90}Y -Janus-DOTA obtained from the fitted exponential functions describing the biodistribution of the injected dose. A summary of the AD (cGy) per megabecquerel injected ^{90}Y for tumor and organs is shown in Figure 2. Note that the tumor had a much greater AD per injected dose (cGy/MBq), which was highly significant compared with all other tissue ($P < 0.01$, ANOVA, Dunnett). The therapeutic ratios (TRs) defined as AD tumor/AD tissue are shown in Figure 3. Note the large TRs for both blood and bone.

DISCUSSION

The mAb from clone 2D12.5 was used because it had the highest 24-h whole-body retention of ^{88}Y -DOTA caused by a high affinity for Y(III)-DOTA ($K_a = 10^8$ mol/L). After intravenous injection in mice, uncomplexed ^{88}Y -, ^{111}In -, and ^{67}Ga -labeled DOTA were all excreted rapidly in the urine. The half-life for elimination was approximately 40 min; $>93\%$ of the injected dose was excreted by the kidneys in 24 h (17).

Our model showed a rapid uptake of the ^{88}Y -Janus-DOTA (C_{max} at t_{max} of 0.4 h) into the leaky neovasculature of the tumor as the injected metal-DOTA was distributed rapidly into the interstitial water (Fig. 1B). Figure 1A is a plot of the %ID/g blood versus time after intravenous in-

jection of ^{111}In - and ^{88}Y -Janus-DOTA 1 h after injection of the polyvalent hapten-protein conjugate. Rapid blood clearance was seen with both ^{88}Y - and ^{111}In -Janus-DOTA.

Previously, we had shown that rapid lowering (chase) of a long-circulating protein was possible by the intravenous injection of a specific antibody (19). In these experiments, the chase of 2D12.5 by injection of the polyvalent hapten-protein conjugate also rapidly lowered the circulating mAb concentration. This procedure had a striking effect on the whole-body 24-h retention of the metal-DOTA injected soon after. When the chase was administered to 20-h pre-targeted mice 1 h before ^{88}Y -DOTA injection, whole-body retention of the metal-chelate fell from $>80\%$ (no chase) to approximately 10% at 3 h and approximately 5% at 24 h after injection of the tracer.

As a matching isotope for ^{90}Y , ^{111}In has been the nuclide of choice because of the similarities in its metabolic handling and coordination chemistry (24). Comparative studies with ^{111}In or ^{90}Y radiolabeled compounds have shown similar pharmacokinetic behavior of the two species (25). Moreover, nitrobenzyl-DOTA binds both yttrium and indium with high stability (26). On the basis of these reports showing that the physicochemical properties of the metal-DOTA are determined primarily by the chelate and not the metal ligand, the ^{111}In - and ^{88}Y -DOTA biodistribution data were pooled.

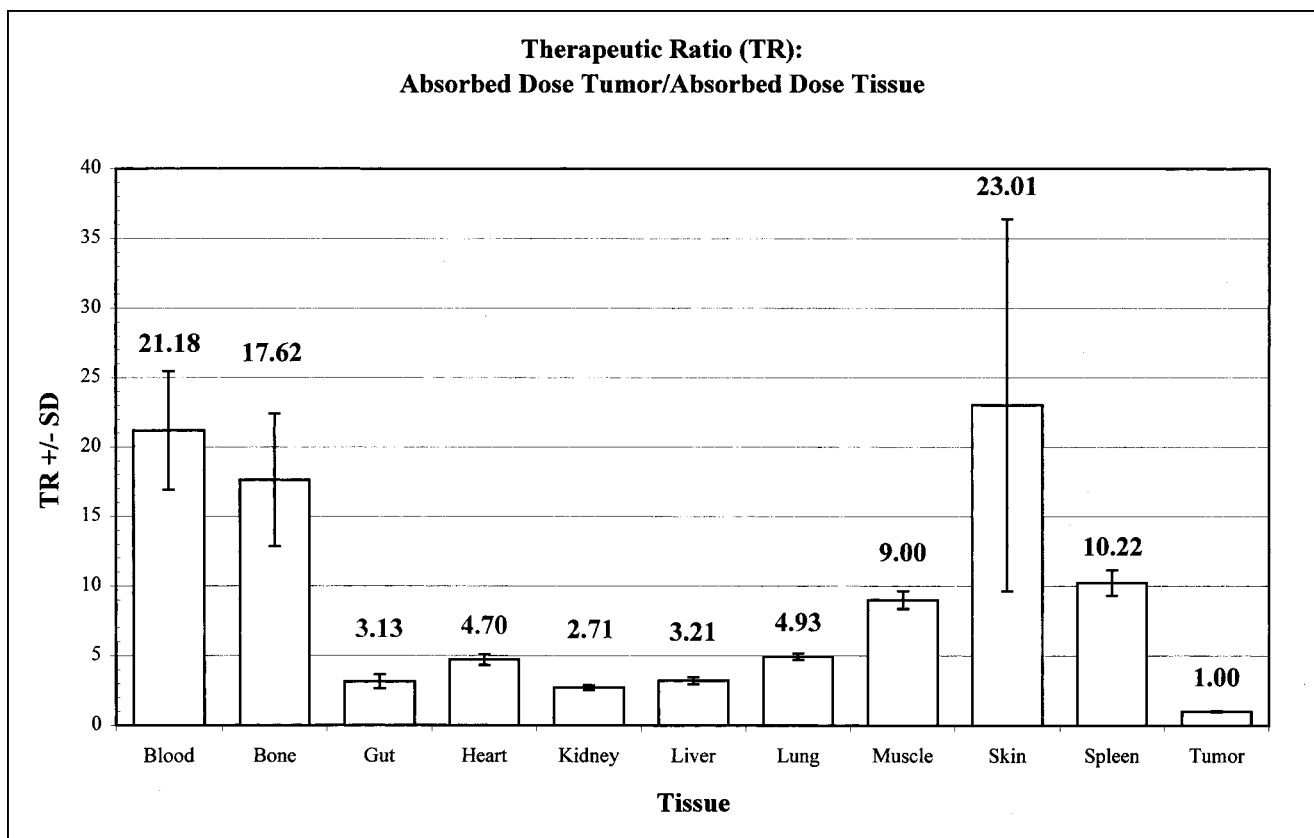


FIGURE 3. Summary of TRs calculated as AD tumor/AD tissue. Note large TRs for blood and bone.

Pretargeting involves the administration of a long-circulating targeted macromolecule (mAb) having a high-affinity noncovalent binding site for a small, rapidly excreted effector molecule, which is given after the mAb has concentrated in the targeted tumor (20). Efficient removal of the hapten-binding macromolecule (mAb) from the circulation with a polyvalent chase macromolecule before giving the effector molecule greatly improves the target-to-blood ratio. Pretargeting without the chase step requires a long waiting period for the blood mAb concentration to fall to very low levels, because even small amounts of mAb remaining in the blood will immediately bind effector molecules on injection. To ensure free effector molecules for diffusion into the tumor and filtration and excretion by the kidneys, circulating mAb must be either saturated or removed. The aggregated mAb produced by cross-linking with the chase in the circulation is endocytosed rapidly by the reticuloendothelial cells, mostly in the liver (18). The intracellular location of the endocytosed mAb prevents the access and binding of a subsequently injected hydrophilic effector molecule. The chase quickly reduces the blood mAb to a very low level so that radioactivity can be administered within 1 h (27).

After injection of the effector molecule (radiolabeled hapten) 1 h after the chase molecule, maximum tumor concentration and tumor-to-normal-tissue ratios were achieved rapidly, and radioactivity was retained in the tumor for several days. The rapid elimination of unlocalized

radioactivity greatly decreased radiation exposure to normal tissue, especially the bone marrow (Figs. 1B and 2). Thus, the pharmacokinetics of the effector molecules gave fast tumor uptake (minutes), slow tumor washout (days), and relatively fast washout from most organs (Figs. 1B and 2, Table 1). This result provided high tumor-to-background ratios and high TRs, which will improve both imaging and radioimmunotherapy (Figs. 2 and 3).

Rapid diffusion, exclusive renal excretion, and extracellular fluid distribution are among the chemical and physiologic properties of an effector molecule that are necessary for achieving the best pretargeting results (26). Our experimental determination of the apparent V_D of 3.3 mL for the metal-DOTA was consistent with literature estimates of the extracellular fluid in the mouse (28). This result, combined with the net negative charge and hydrophilic nature of the metal-hapten, suggested that the metal-DOTA was confined essentially to the extracellular volume with very little intracellular uptake (29).

Rapid uptake of the metal-DOTA by both tumor and organs seen in our model (Figs. 1A and B) with a C_{max} at approximately 0.4 h was consistent with rapid distribution of the metal-DOTA into the interstitial water. Clearance of the metal-DOTA from the tumor was slow compared with that of blood, because the metal-DOTA was bound to the pretargeted antibody (Fig. 1A).

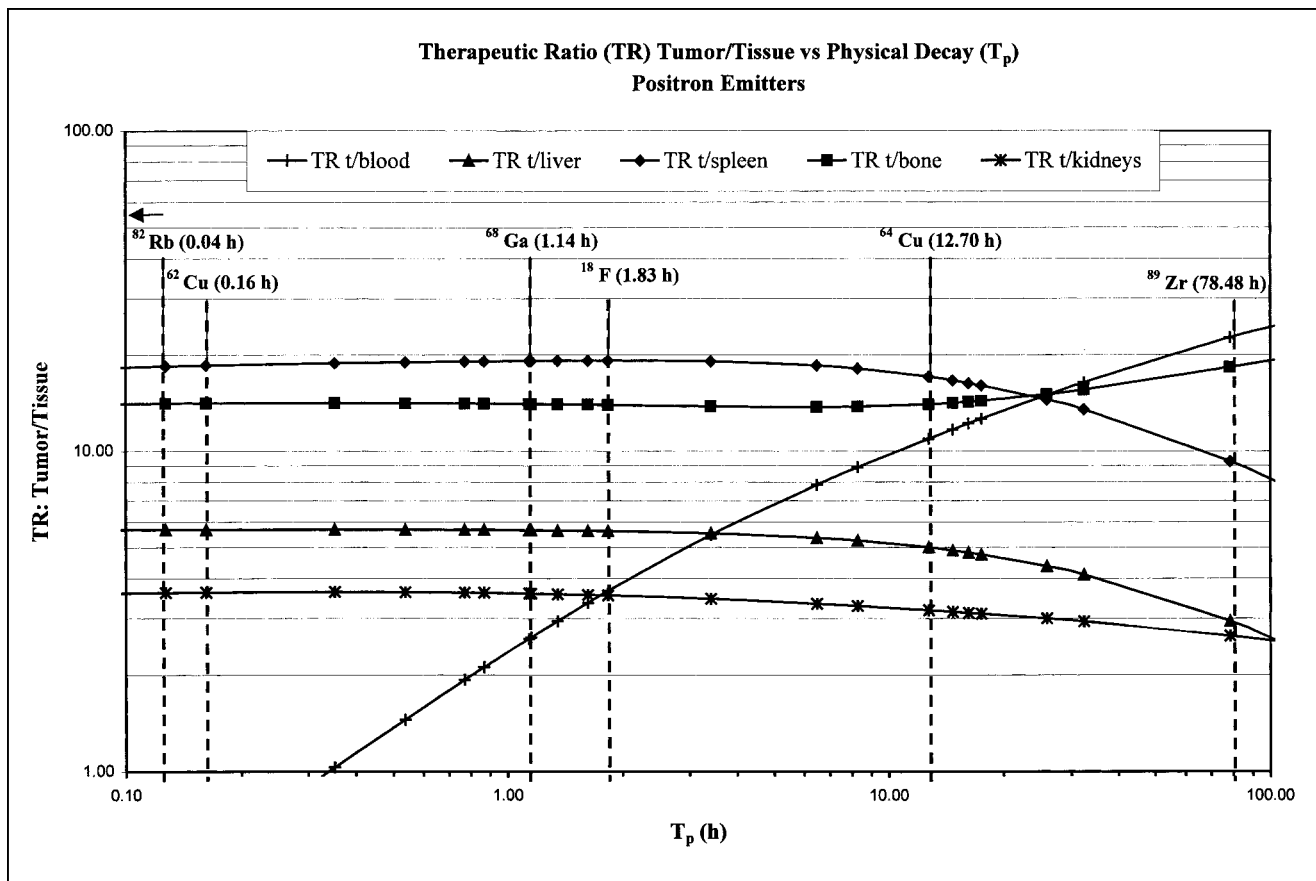


FIGURE 4. Summary plot of several tumor-to-tissue TRs vs. T_p for select number of positron-emitting radionuclides.

From the tumor and organ time-integrated radioactivity (^{90}Y MBq \times s/kg) and AD (cGy) for ^{90}Y -Janus-DOTA, the tumor had the largest AD compared with all other tissue (Fig. 2, Table 2). Moreover, TRs were $>2.5/1$ for all measured tissue (Fig. 3); TRs for both blood (21/1) and bone (18/1) were particularly dramatic. The tumor-to-blood TR of $>20/1$ was much greater than the 2–3/1 obtained with directly labeled mAb (1). This large gain in the tumor-to-blood TR is highly desirable for both radioimmunodetection and radioimmunotherapy.

Radiation dose is related to the effective retention of activity in tissue (T_e), reflecting both radioactive decay and biologic clearance processes (30). Biologic retention and clearance values are best characterized by the AUC (%ID \times h/g tissue) obtained from the integration of the equation describing the %ID/g tissue (obtained from a suitable tracer) as a function of time (Eq. 1) and is given by the following relationship:

$$\text{AUC}_{0 \rightarrow \infty} = \sum A_j / \lambda_j, \quad \text{Eq. 12}$$

where A_j (%ID/g tissue) and λ_j (biologic decay and uptake rate constants, h^{-1}) are obtained from the fit of Equation 1. Cumulative activity in tissue is derived from the decay-corrected tissue count data and T_p of the radionuclide and is best characterized by the AUC (MBq \times s/kg tissue) ob-

tained from the integration of Equation 4. Cumulated activity in tissue is given by the following relationship:

$$\text{AUC}_{0 \rightarrow \infty} = c_1 \sum A_j / (\lambda_j + \lambda_p), \quad \text{Eq. 13}$$

where c_1 is a constant for the conversion of %ID/g to MBq/kg and λ_p is the radionuclide decay constant (time^{-1}) (Eq. 7).

As a first approximation, the AD is related to the cumulative activity in a specific tissue (Eq. 8). For several reasons, the dose is not directly proportional to cumulated activity. Some of the energy emitted from radionuclides in an organ or tissue may be imparted to more distant organs or may completely escape the body. Moreover, accurate AD calculations also depend on the size and shape of the organ and the density and atomic composition of the tissue (30). In a mouse model, Hui et al. (31) and Beatty et al. (32) showed that the dosimetry calculation model, using the standard assumption for humans that all β -energy is deposited within the organs or tumor in which it is localized, is inadequate for determining the β -AD for mouse organs. Because the tumors in our mouse model weighed significantly more, we estimated the self-absorbed fraction to be approximately 0.5 for our tumors. Thus, the actual dose to our tumors is probably closer to half the value we calculated using standard assumptions. On the other hand, we did not consider

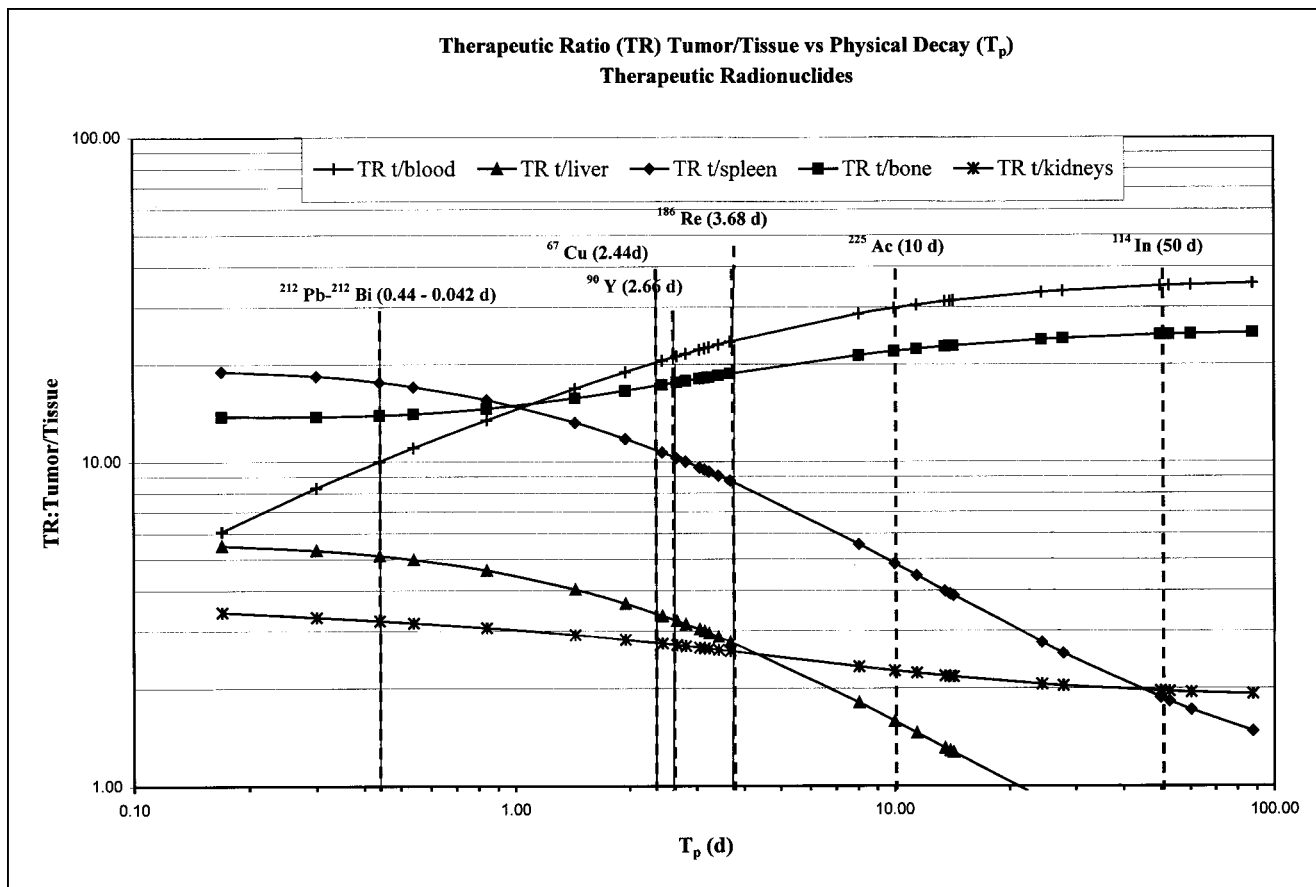


FIGURE 5. Summary plot of several tumor-to-tissue TRs vs. T_p for various therapeutic radionuclides.

the dose caused by β -particles entering from adjacent tissue or as circulating activity, which is lower with pretargeting than with conventional radioimmunotherapy. Although the mouse dosimetry is overestimated, the uncorrected values should apply to larger human organs (17).

It is likely, as shown for ^{111}In , ^{88}Y , and ^{90}Y , that the biodistribution and biologic half-life (T_b) of many other metal-DOTA chelates will be very similar if not identical (33). Thus, the relative AD for each radiometal to the organs and the tumor should be directly proportional to the T_p for that radionuclide. Plotting several TRs as a function of T_p (Figs. 4 and 5) for various imaging and therapeutic radionuclides, we notice that the tumor-to-liver TR is <1 for radionuclides with half-lives >10 d. The reason for this result is suggested by a careful analysis of the biodistribution data for the liver. Although the absolute %ID/g is small for the liver, the radionuclide-DOTA-mAb complex is not cleared readily and thus has a very long biologic half-life compared with other tissue (Fig. 1B). Thus, for therapeutic radionuclides with $T_p > 10$ d, the T_e of the complex in the liver is quite pronounced, with more energy imparted to the liver than to the tumor. Similarly, for radionuclides with $T_p < 1$ h, the TR decreases rapidly, especially for the blood and gut.

CONCLUSION

The high tumor uptake of ^{90}Y -DOTA and subsequent high radioactivity, coupled with low radioactivity in bone, blood, and other organs, suggests that a three-step pretargeting protocol has considerable promise as a method for ^{90}Y -radioimmunotherapy.

ACKNOWLEDGMENTS

This study was supported in part by the Medical Research Service of the Department of Veterans Affairs (Program 821 Merit Review and special program support) (DAG and MH) and PHS grant numbers CA 28343 and CA 48282 (DAG) and CA 16861 (CFM).

REFERENCES

1. Goldenberg DM, Kim EE, Bennett SJ, Nelson MO, Deland FH. Carcinoembryonic antigen radioimmunodetection in the evaluation of colorectal cancer and in the detection of occult neoplasms. *Gastroenterology*. 1983;84:524-532.
2. DeNardo SJ, DeNardo GL, Peng J-S, Colcher D. Monoclonal antibody radiopharmaceuticals for cancer radioimmunotherapy. In: Burchiel S, Rhodes B, eds. *Radioimmunoimaging and Radioimmunotherapy*. New York, NY: Elsevier; 1983:409-417.
3. Halpern SE, Hagan PL, Garver PR, et al. Stability, characterization, and kinetics of ^{111}In -labeled monoclonal antitumor antibodies in normal animals and nude mouse-human tumor models. *Cancer Res*. 1983;43:5347-5355.

4. Bloomer WD, Lipsztein R, Dalton JF. Antibody-mediated radiotherapy. *Cancer*. 1985;55:2229–2233.
5. Meares CF, Moi MK, Diril H, et al. Macrocyclic chelates of radiometals for diagnosis and therapy. *Br J Cancer*. 1990(suppl);10:21–26.
6. Meares CF, McCall MJ, Reardan DT, Goodwin DA, Diamanti CI, McTigue M. Conjugation of antibodies with bifunctional chelating agents: isothiocyanate and bromoacetamide reagents, methods of analysis, and subsequent addition of metal ions. *Anal Biochem*. 1984;142:68–78.
7. Douillard JY, Lehur PA, Aillet G, et al. Immunohistochemical antigenic expression and in vivo tumor uptake of monoclonal antibodies with specificity for tumors of the gastrointestinal tract. *Cancer Res*. 1986;46:4221–4224.
8. Goodwin DA. Pharmacokinetics and antibodies. *J Nucl Med*. 1987;28:1358–1362.
9. Fairweather DS, Bradwell AR, Dykes PW, Vaughan AT, Watson-James SF, Chandler S. Improved tumour localisation using indium-111 labelled antibodies. *BMJ (Clin Res Ed)*. 1983;287:167–170.
10. Chatal JF, Fumoleau P, Saccavini JC, et al. Immunoscintigraphy of recurrences of gynecologic carcinomas. *J Nucl Med*. 1987;28:1807–1819.
11. Press OW, Eary JF, Appelbaum FR, et al. Radiolabeled-antibody therapy of B-cell lymphoma with autologous bone marrow support. *N Engl J Med*. 1993;329:1219–1224.
12. Wessels BW, Rogus RD. Radionuclide selection and model absorbed dose calculations for radiolabeled tumor associated antibodies. *Med Phys*. 1984;11:638–645.
13. Lee YC, Washburn LC, Sun TT, et al. Radioimmunotherapy of human colorectal carcinoma xenografts using ⁹⁰Y-labeled monoclonal antibody CO17-1A prepared by two bifunctional chelate techniques. *Cancer Res*. 1990;50:4546–4551.
14. Moi MK, Meares CF, DeNardo SJ. The peptide way to macrocyclic bifunctional chelating agents: synthesis of 2-(p-nitrobenzyl)-1,4,7,10-tetraazacyclododecane-N,N',N'',N'''-tetraacetic acid and the study of its yttrium (III) complex. *J Am Chem Soc*. 1988;110:6266–6267.
15. Renn O, Meares CF. Large-scale synthesis of the bifunctional chelating agent 2-(p-nitrobenzyl)-1,4,7,10-tetraazacyclododecane-N,N',N'',N'''-tetraacetic acid, and the determination of its enantiomeric purity by chiral chromatography. *Bioconj Chem*. 1992;3:563–569.
16. DeNardo SJ, Kukis DL, Miers LA, et al. Yttrium-90-DOTA-peptide-chimeric L6 radioimmunoconjugate: efficacy and toxicity in mice bearing p53 mutant human breast cancer xenografts. *J Nucl Med*. 1998;39:842–849.
17. Goodwin DA, Meares CF, Watanabe N, et al. Pharmacokinetics of pretargeted monoclonal antibody 2D12.5 and ⁸⁸Y-Janus-2-(p-nitrobenzyl)-1,4,7,10-tetraazacyclododecanetetraacetic acid (DOTA) in BALB/c mice with KHJJ mouse adenocarcinoma: a model for ⁹⁰Y radioimmunotherapy. *Cancer Res*. 1994;54:5937–5946.
18. Goodwin DA, Meares CF, McCall MJ, McTigue M, Chaovapong W. Pre-targeted immunoscintigraphy of murine tumors with indium-111-labeled bifunctional haptens. *J Nucl Med*. 1988;29:226–234.
19. Goodwin D, Meares C, Diamanti C, et al. Use of specific antibody for rapid clearance of circulating blood background from radiolabeled tumor imaging proteins. *Eur J Nucl Med*. 1984;9:209–215.
20. Goodwin DA. Tumor pretargeting: almost the bottom line [editorial]. *J Nucl Med*. 1995;36:876–879.
21. Axworthy DB, Reno JM, Hylarides MD, et al. Cure of human carcinoma xenografts by a single dose of pretargeted yttrium-90 with negligible toxicity. *Proc Natl Acad Sci U S A*. 2000;97:1802–1807.
22. Goodwin DA, Sundberg MW, Diamanti CI, Meares CF. Indium radiopharmaceuticals in cancer localization. In: Haynie T, ed. *Radiologic and Other Biophysical Methods in Tumor Diagnosis*. Houston, TX: Yearbook Medical Publishers; 1975:57–88.
23. Dunnett CW, Gent M. Significance testing to establish equivalence between treatments, with special reference to data in the form of 2 × 2 tables. *Biometrics*. 1977;33:593–602.
24. Camera L, Kinuya S, Garmestani K, et al. Comparative biodistribution of indium- and yttrium-labeled B3 monoclonal antibody conjugated to either 2-(p-SCN-Bz)-6-methyl-DTPA (1B4M-DTPA) or 2-(p-SCN-Bz)-1,4,7,10-tetraazacyclododecane tetraacetic acid (2B-DOTA). *Eur J Nucl Med*. 1994;21:640–646.
25. Cremonesi M, Ferrari M, Chinol M, et al. Three-step radioimmunotherapy with yttrium-90 biotin: dosimetry and pharmacokinetics in cancer patients. *Eur J Nucl Med*. 1999;26:110–120.
26. Goodwin DA, Meares CF, Osen M. Biological properties of biotin-chelate conjugates for pretargeted diagnosis and therapy with the avidin/biotin system. *J Nucl Med*. 1998;39:1813–1818.
27. Goodwin DA, Meares CF. Pretargeting: general principles; October 10–12, 1996. *Cancer*. 1997;80:2675–2680.
28. Baxter LT, Zhu H, Mackensen DG, Jain RK. Physiologically based pharmacokinetic model for specific and nonspecific monoclonal antibodies and fragments in normal tissues and human tumor xenografts in nude mice. *Cancer Res*. 1994;54:1517–1528.
29. Denardo SJ, Richman CM, Goldstein DS, et al. Yttrium-90/indium-111-DOTA-peptide-chimeric L6: pharmacokinetics, dosimetry and initial results in patients with incurable breast cancer. *Anticancer Res*. 1997;17:1735–1744.
30. Badger CC, Fisher DR. The importance of accurate radiation dosimetry in radioimmunotherapy of cancer [editorial]. *J Nucl Med*. 1994;35:300–302.
31. Hui TE, Fisher DR, Kuhn JA, et al. A mouse model for calculating cross-organ beta doses from yttrium-90-labeled immunoconjugates. *Cancer*. 1994;73:951–957.
32. Beatty BG, Kuhn JA, Hui TE, Fisher DR, Williams LE, Beatty JD. Application of the cross-organ beta dose method for tissue dosimetry in tumor-bearing mice treated with a ⁹⁰Y-labeled immunoconjugate. *Cancer*. 1994;73:958–965.
33. DeNardo GL, Kroger LA, Meares CF, et al. Comparison of 1,4,7,10-tetraazacyclododecane-N,N',N'',N'''-tetraacetic acid (DOTA)-peptide-ChL6, a novel immunoconjugate with catabolizable linker, to 2-iminothiolane-2-[p-(bromoacetamido)benzyl]-DOTA-ChL6 in breast cancer xenografts. *Clin Cancer Res*. 1998;4:2483–2490.